

A Test to Evaluate the Performance of Aromaticity Descriptors in All-Metal and Semimetal Clusters. An Appraisal of Electronic and Magnetic Indicators of Aromaticity

Ferran Feixas,[†] J. Oscar C. Jiménez-Halla,[†] Eduard Matito,[‡] Jordi Poater,[†] and Miquel Solà^{*,†}

Institut de Química Computacional and Departament de Química, Universitat de Girona, Campus de Montilivi, 17071 Girona, Catalonia, Spain and Institute of Physics, University of Szczecin, 70-451 Szczecin, Poland

Received January 19, 2010

Abstract: As compared to classical organic aromatic compounds, the evaluation of aromaticity in all-metal and semimetal clusters is much more complex. For a series of these clusters, it is frequently found that different methods used to discuss aromaticity lead to divergent conclusions. For this reason, there is a need to evaluate the reliability of the different descriptors of aromaticity to provide correct trends in all-metal and semimetal aromatic clusters. This work represents the first attempt to assess the performance of aromaticity descriptors in all-metal clusters. To this end, we introduce the series of all-metal and semimetal clusters $[X_nY_{4-n}]^{q\pm}$ ($X, Y = Al, Ga, Si$, and Ge ; $n = 0–4$) and $[X_nY_{5-n}]^{4–n}$ ($X = P$ and $Y = S$ and Se ; $n = 0–5$) with predictable aromaticity trends. Aromaticity, in these series, is quantified by means of nucleus-independent chemical shifts (NICS) and electronic multicenter indices (MCI). Results show that the expected trends are generally better reproduced by MCI than by NICS. It is found that $NICS(0)_\pi$ is the kind of NICS that performs better among the different NICS indices analyzed.

1. Introduction

The discovery of aromaticity in Al_4^{2-} ,¹ an all-metal inorganic cluster, in 2001 by Boldyrev, Wang, and co-workers fuelled the interest for the study of all-metal and semimetal inorganic clusters with aromatic properties (for three recent reviews see ref 2). At variance with the classical aromatic organic molecules that possess only π -electron delocalization, the aromaticity in inorganic clusters is more complex due to the peculiarities of chemical bonding in metal systems. These metal compounds present σ -, π -, and δ -³ or even ϕ -⁴ electron delocalization, thus, giving rise to the so-called multifold aromaticity/antiaromaticity^{2,5} as well as cases of conflicting aromaticity.^{2a,6}

Most of the methods to quantify aromaticity have been developed for the classical aromatic organic molecules, and they cannot be applied to inorganic clusters without further reinvestigation. This is the case, among others, of the harmonic oscillator model of aromaticity (HOMA)⁷ or the aromatic fluctuation (FLU)⁸ indicators of aromaticity that take benzene, the paradigmatic aromatic molecule, or other aromatic organic molecules as a reference in their definitions. Likewise, resonance energies (RE) or aromatic stabilization energies (ASE)⁹ are very difficult to compute accurately in all-metal clusters because of the lack of appropriate reference systems.^{5c,10} For the moment, the most widely used methods to discuss aromaticity in all-metal clusters have been the simple electron counting based on the $4n + 2$ Hückel's rule¹¹ and the calculation of the nucleus-independent chemical shifts (NICS).¹² Less common is the use of electronic multicenter indices (MCI),¹³ for which few examples can be found in the literature.¹⁴

* Corresponding author: Tel.: +34.972.41.89.12; Fax: +34.972.41.83.56; E-mail address: miquel.sola@udg.edu.

[†] University of Szczecin.

[‡] Universitat de Girona.

Although the $4n + 2$ rule affords the simple test of aromaticity, electron counting alone does not provide always direct evidence of aromaticity/antiaromaticity.^{2c,15} For instance, Al_4^{2-} contains one pair of delocalized π -electrons and two pairs of σ -electrons that contribute to the overall aromaticity of this species.^{1,6a,16} The two π -electrons obey the $4n + 2$ Hückel's rule for monocyclic's π -systems. Although this is not the case for the four σ -electrons, it was found that the two pairs of delocalized σ electrons belong to molecular orbitals (MOs) that follow orthogonal radial and tangential directions, which makes them totally independent,¹⁷ thus, separately following the $4n + 2$ rule. This is a clear example that simple total electronic counts sometimes lead to erroneous conclusions.^{2c,15} Similarly, in planar polycyclic boron clusters, it has been found that the aromaticity is not related to the total number of π -electrons.¹⁸

Probably the most widely employed method to analyze the aromaticity of all-metal species is the NICS index. This descriptor, proposed by Schleyer and co-workers¹² as a magnetic index of aromaticity, is a valuable indicator of aromaticity that is used by many researchers. It is defined as the negative value of the absolute shielding computed at a ring center or at some other interesting point of the system, usually 1 Å above the ring center. Rings with large negative NICS values are considered aromatic. The more negative the NICS values, the more aromatic the rings are. Nonaromatic species have NICS values close to zero, and positive NICS values are indicative of antiaromaticity. Recently, dissected NICS techniques based on the analysis of individual canonical MOs contributions to NICS¹⁹ have been successfully applied to analyze multifold and conflicting aromaticity/antiaromaticity in all-metal clusters.²⁰

In a recent work, some of us reported that NICS profiles calculated in the perpendicular direction of each ring are useful to classify all-metal and semimetal clusters into three groups according to their aromatic, nonaromatic, or antiaromatic character.²¹ In addition, Tsipis has recently demonstrated that the NICS _{∞} -scan patterns, along with symmetry-based selection rules, can unequivocally probe the antiaromaticity in a wide range of antiaromatic organic and inorganic rings/cages.²² We also showed²¹ that single-point NICS calculations fail to provide correct trends for some particular systems. For example, we found unexpectedly that C_{2v} GeAl_3^- is more aromatic than D_{4h} Al_4^{2-} , according to NICS(0) values.²¹ In another work, we discovered that the NICS and MCI predicted changes of aromaticity in Mg_3^{2-} when coordinated to alkali metal cations follow opposite trends.^{14c} Similar results were reported by Chattaraj et al. for the metal complexation of Al_4^{2-} .^{14b} The reason for the divergence between NICS and MCI is unclear in some cases. The connection between these indicators is not obvious because NICS values are computed as a response to an external magnetic field, and virtual orbitals are involved in the calculation, while in the computation of electron sharing indices (ESI), such as MCI, only occupied orbitals are used. In fact, it is well-known that a delocalized system is a necessary but not a sufficient condition to have a ring current.^{14a,23}

In a subsequent work,²⁴ we introduced a series of 15 aromaticity tests that can be used to analyze the advantages and the drawbacks of a group of aromaticity descriptors. Based on the results obtained for a set of 10 indicators of aromaticity, including NICS and MCI, we concluded that MCI were the most accurate among all indices examined in that work.²⁴ In addition, the fact that the π -component of the four center-electron index in Al_4^{2-} is almost the same as that of $\text{C}_4\text{H}_4^{2+}$ seems to indicate an apparent good behavior of MCI for all-metal clusters.^{14a} The 15 tests of aromaticity proposed in the previous work²⁴ involved only classical aromatic molecules, having expected aromaticity trends based on accumulated chemical experience. In the present work, we introduce a new test containing several inorganic all-metal clusters with two main aims: first, to investigate the performance of NICS and MCI to provide expected aromaticity trends in all-metal clusters; and second, to analyze whether, among different NICS definitions, there is a particular NICS index that performs consistently better than the rest.

To this end, we have chosen the four-membered ring (4-MR) series of valence isoelectronic inorganic species $[\text{X}_n\text{Y}_{4-n}]^{q\pm}$ ($\text{X}, \text{Y} = \text{Al}, \text{Ga}, \text{Si}, \text{and Ge}; n = 0-4$) that have a predictable trend of aromaticity. Thus, one can predict a steep decrease in aromaticity when going from Al_4^{2-} to, for instance, GeAl_3^- due to the reduction of symmetry and to the substitution of one Al atom by a more electronegative Ge atom. A smooth reduction of aromaticity when going from Al_3Ge^- to Al_2Ge_2 is also likely, although more arguable. And the same should occur from Ge_4^{2+} to Al_2Ge_2 . Therefore, for instance, the expected order of aromaticity in one ($\text{X} = \text{Al}$ and $\text{Y} = \text{Ge}$) of the six series chosen is $\text{Al}_4^{2-} > \text{Al}_3\text{Ge}^- \geq \text{Al}_2\text{Ge}_2 \leq \text{AlGe}_3^+ < \text{Ge}_4^{2+}$. A similar behavior is likely to be present in a series where X and Y come from different groups of the Periodic Table. In the series with $\text{X} = \text{Al}$ and Ga and $\text{Y} = \text{Si}$ and Ge , the electronegativity of X and Y is significantly different and, consequently, large changes in bond distances and angles are observed. On the other hand, when X and Y belong to the same group (for instance, $\text{X} = \text{Al}$ and $\text{Y} = \text{Ga}$), electronegativity and geometrical parameters remain almost unchanged. This fact leads to small changes in the aromaticity and, thus, the expected trend becomes $\text{Al}_4^{2-} \geq \text{Al}_3\text{Ga}^{2-} \sim \text{Al}_2\text{Ga}_2^{2-} \sim \text{AlGa}_3^{2-} \leq \text{Ga}_4^{2-}$. Finally, apart from these series, we have included two $[\text{X}_n\text{Y}_{5-n}]^{4-n}$ ($\text{X} = \text{P}$ and $\text{Y} = \text{S}$ and $\text{Se}; n = 0-5$) series of 5-MRs. It is worth noting that the electronic, molecular structure, and aromaticity of some of the systems studied here have been analyzed in previous theoretical and experimental works (Al_4^{2-} ,^{1,5c,6a,10,14a,b,15a,16,17,23,25} Ga_4^{2-} ,^{10,25a,26} Al_3Si^{-} ,²⁷ Al_2Si_2 ,^{5f,25a,28} AlSi_3 ,^{28b} Si_4^{2+} ,^{5d,28b} Al_3Ge^{-} ,^{27a} Al_2Ge_2 ,^{5f,28a} AlGe_3 ,^{28b} Ge_4^{2+} ,^{28b} Ga_3Si^{-} ,²⁹ Ga_2Si_2 ,^{5f,25a,28} GaSi_3 ,^{28b} Ga_3Ge^{-} ,²⁹ Ga_2Ge_2 ,^{5f,28a} GaGe_3 ,^{28b} $\text{Si}_2\text{Ge}_2^{2+}$,^{28b} and P_5^{-} ,^{5e,30}). It has been found that the elements of the $[\text{X}_n\text{Y}_{4-n}]^{q\pm}$ series present σ - and π -aromaticity, while $[\text{X}_n\text{Y}_{5-n}]^{4-n}$ compounds are only π -aromatic. The present study complements the available experimental and theoretical data, which is scarce or missing for some clusters, and enables a systematic analysis of aromaticity trends along the eight clusters series $[\text{X}_n\text{Y}_{4-n}]^{q\pm}$ ($\text{X}, \text{Y} = \text{Al}, \text{Ga}, \text{Si}, \text{and Ge}$;

$n = 0\text{--}4$) and $[X_nY_{5-n}]^{4-n}$ ($X = \text{P}$ and $\text{Y} = \text{S}$ and Se ; $n = 0\text{--}5$), all obtained with the same methodology.

2. Computational Details

All calculations in this work were performed by means of the Gaussian03³¹ computational package. The gas-phase optimized geometries reported here were calculated in the framework of density functional theory (DFT) using the B3LYP functional,³² which combines the three-parameter Becke's exchange³³ and Lee-Yang-Parr's correlation³⁴ nonlocal functionals. The 6-311+G(d) basis set³⁵ was used for all calculations.

In the present work, we report results for two unstable dianions such as Al_4^{2-} and Ga_4^{2-} . In a recent work, Lambrecht et al.³⁶ have shown that Al_4^{2-} is unstable as compared to $\text{Al}_4^- + \text{free e}^-$ and, consequently, its properties change significantly when increasing the number of diffuse functions in the basis set. Indeed, after inclusion of certain number of diffuse functions, the Al_4^{2-} evolves to $\text{Al}_4^- + \text{free e}^-$. In this sense, Lambrecht and co-workers³⁶ warned about the validity of calculations carried out for such unstable dianions. In a recent comment³⁷ (see also the rebuttal in ref 38) on the work by Lambrecht et al.,³⁶ Zubarev and Boldyrev argued against this point of view and considered that the bound state of the individual Al_4^{2-} is an adequate model of Al_4^{2-} in a stabilizing environment, such as in NaAl_4^- or Na_2Al_4 . They also considered that calculations for isolated Al_4^{2-} species using a 6-311+G(d) basis provide an accurate model for the Al_4^{2-} unit embedded in a stabilizing environment. Following the Zubarev and Boldyrev arguments,³⁷ we will discuss the properties of the bound state in these two metastable dianions by employing the 6-311+G(d) basis set.

NICS values were computed also with the B3LYP/6-311+G(d) method through the gauge-including atomic orbital method (GIAO)³⁹ implemented in Gaussian03. The magnetic shielding tensor was calculated for the ghost atoms located at the ring centers (NICS(0)) determined by the nonweighted mean of the heavy atom coordinates and also for the ring critical point (RCP), the point of lowest density in the ring plane,⁴⁰ as suggested by Cossío et al.,⁴¹ to yield NICS(0)^{rCP} values. In some high-symmetry molecules both points, the ring center and the RCP, coincide. In addition, NICS has been also calculated at 1 Å above the molecular plane of the ring (NICS(1) and NICS(1)^{rCP}).⁴² NICS(1) is considered to better reflect the π -electron effects than that of NICS(0). The out-of-plane tensor component of NICS (NICS(0)_{zz}, NICS(0)_{zz}^{rCP}, NICS(1)_{zz}, and NICS(1)_{zz}^{rCP}) have also been collected. This latter quantity gives probably the best measure of aromaticity among the different NICS-related definitions in organic molecules.^{24,43} Moreover, NICS(0) _{π} , NICS(0) _{π} ^{rCP}, NICS(0) _{σ} , and NICS(0) _{σ} ^{rCP} have been obtained from the decomposition of NICS into its MO components using the NBO 5.0 program.⁴⁴ For these calculations, only the contributions of valence orbitals have been taken into account. The dissected NICS methods have already been widely applied to analyze multifold aromaticity in all-metal clusters.²⁰

For the aromaticity analysis, we have also applied the MCI.^{13b,c} MCI is a particular extension of the I_{ring} index:^{13a}

$$I_{\text{ring}}(A) = \sum_{i_1, i_2, \dots, i_N} n_{i_1}, \dots, n_{i_N} S_{i_1 i_2}(A_1) S_{i_2 i_3}(A_2), \dots, S_{i_N i_1}(A_N) \quad (1)$$

n_i is the occupancy of MO i and $S_{ij}(A)$ is the overlap between MOs i and j within the molecular space assigned to atom A . Summing up all the I_{ring} values resulting from the permutations of indices A_1, A_2, \dots, A_N , the mentioned MCI index^{13c} is defined as

$$\text{MCI}(A) = \frac{1}{2N} \sum_{P(A)} I_{\text{ring}}(A) \quad (2)$$

where $P(A)$ stands for a permutation operator which interchanges the atomic labels A_1, A_2, \dots, A_N to generate up to the $N!$ permutations of the elements in the string A .^{13b,45} MCI and I_{ring} give an idea of the electron sharing between all atoms in the ring. The more positive the MCI values,^{13c,46} the more aromatic the rings. For planar species, as those treated in the present work, $S_{\sigma\pi}(A) = 0$ and both MCI and I_{ring} can be exactly split into the σ - and π -contributions. This feature is especially interesting to evaluate multifold aromaticity in all-metal clusters. Finally, although several atomic partitions may be used for the calculations of the overlap between MOs i and j within the molecular space assigned to atom A ,^{14a,47} we have chosen in the present work the partition carried out in the framework of the quantum theory of atoms-in-molecules (QTAIM) of Bader,^{40,48} by which atoms are defined from the condition of zero-flux gradient in the one-electron density, $\rho(\mathbf{r})$. Calculation of atomic overlap matrices (AOM) and computation of MCI have been performed with the AIMPA⁴⁹ and ESI-3D⁵⁰ collection of programs.⁵¹ Since MCI and I_{ring} yield very similar results, in this work, we report only MCI values.

3. Results and Discussion

In this section, we first discuss the series $[\text{Al}_n\text{Ge}_{4-n}]^{2-n}$ ($n = 0\text{--}4$) in detail. Then the results for the rest of the $[\text{X}_n\text{Y}_{4-n}]^{q\pm}$ series are briefly analyzed. Finally, the molecular structure and aromaticity of the $[\text{X}_n\text{Y}_{5-n}]^{4-n}$ ($X = \text{P}$ and $\text{Y} = \text{S}$ and Se ; $n = 0\text{--}5$) clusters are presented.

Table 1 contains the molecular structure and the MCI and NICS results obtained for the series $[\text{Al}_n\text{Ge}_{4-n}]^{2-n}$ ($n = 0\text{--}4$). The number of valence electrons is 14 for all members of the series. The molecular structure of the ground state of Al_4^{2-} and Ge_4^{2+} clusters is D_{4h} square planar.^{28b} The geometry of the ground state of Al_3Ge^- ^{27a} and AlGe_3^+ ^{28b} clusters is a planar distorted rhombus of C_{2v} symmetry. It is worth noting that in the case of heteroatoms having substantially different electronegativities, as in Al_3C^- , the most stable molecular structure becomes the C_{3v} pyramidal.^{27a} This can be likely attributed to the loss of aromaticity due to higher electronegativity differences. For Al_2Ge_2 , there are two possible planar structures corresponding to the *cis* and *trans* configurations.^{5f,28a} According to previous studies, the Al_2Ge_2 cluster is more stable in the *trans* configuration,^{5f,28b} while the *cis* is the most stable configuration for Ga_2Ge_2 ,^{5f,28b} Al_2Si_2 ,^{5f,25a,28b} and Ga_2Si_2 .^{5f,28b} In order to make comparisons between different series easier,

Table 1. Molecular Structure and Values of the MCI, MCI_{π} , and MCI_{σ} (in electrons) and the NICS (in ppm) Indices^a

	Al_4^{2-}	Al_3Ge^-	Al_2Ge_2	$AlGe_3^+$	Ge_4^{2+}
Symmetry	D_{4h}	C_{2v}	C_{2v}	C_{2v}	D_{4h}
MCI	0.356	0.206	0.165	0.171	0.386
MCI_{π}	0.187	0.114	0.102	0.128	0.187
MCI_{σ}	0.169	0.092	0.063	0.043	0.199
NICS(0)	-34.45	-34.57	-35.00	-38.18	-42.20
NICS(0) ^{cp}	-34.45	-31.98	-30.00	-31.90	-42.20
NICS(1)	-27.39	-26.97	-26.56	-28.72	-30.28
NICS(1) ^{cp}	-27.39	-25.66	-24.16	-25.73	-30.28
NICS(0) _{zz}	-66.14	-64.09	-64.68	-67.84	-69.36
NICS(0) _{zz} ^{cp}	-66.14	-62.75	-62.88	-66.10	-69.36
NICS(1) _{zz}	-54.85	-53.66	-53.65	-57.31	-58.56
NICS(1) _{zz} ^{cp}	-54.85	-52.59	-52.11	-55.36	-58.56
NICS(0) _{π}	-21.72	-20.95	-20.32	-22.71	-24.31
NICS(0) _{π} ^{cp}	-21.72	-19.82	-18.02	-19.40	-24.31
NICS(0) _{σ}	-12.23	-12.62	-13.36	-13.79	-16.23
NICS(0) _{σ} ^{cp}	-12.23	-11.25	-10.78	-10.94	-16.23

^a Calculated at the ring center and at the ring critical point (RCP) for the series Al_4^{2-} , Al_3Ge^- , Al_2Ge_2 , $AlGe_3^+$, and Ge_4^{2+} at the B3LYP/6-311+G(d) level of theory.

in all cases, we have taken the *cis* configuration for the $X_2Y_2^{q\pm}$ species, despite, in some cases, the *trans* configuration is the most stable. Aromatic ring current shielding (ARCS) results from Jusélius et al. indicate that the aromaticity of the *cis* and *trans* configurations is similar in Al_2Si_2 .^{25a}

The MCI and MCI_{π} values obtained for Al_4^{2-} are 0.356 and 0.187 e, respectively, not far from the values, 0.341 and 0.161 e, reported by Mandado et al.^{14a} with the same QTAIM partition of the molecular space and with the same B3LYP/6-311+G(d) methodology.⁵² The value of the MCI_{π} can be easily and analytically obtained for any ring X_4 of D_{4h} symmetry with only two π -electrons occupying the same orbital, such as in Al_4^{2-} . Following the procedure that we applied to get analytical delocalization indices for two π -electron cyclic systems,⁵³ in Al_4^{2-} there is a single π -orbital involved in the sum of eq 1, and the self-overlap of this π -orbital in a given basin is by construction $S_{\pi\pi}(A) = 1/4$. Application of eq 2 yields a MCI value of $3/16 = 0.1875$ e, which is independent of the basis set used for the calculation (it can differ only if correlated wave functions are used).^{47a} On the other hand, Mandado et al.^{14a} and Roy et al.^{14b} reported total MCI values of 0.335 and 0.313 e, respectively, both calculated with the same methodology used in the present work but using Mulliken instead of QTAIM partition. This shows that the effect of using different partitions for the calculation of MCI is minor in the case of Al_4^{2-} . Our results also point out that the π delocalization in the Al_4^{2-} species is slightly larger than that of the σ (0.187 vs 0.169 e). This is in line with previous dissected NICS results,^{14a} showing that $NICS(0)_{\pi}$ is somewhat more negative than $NICS(0)_{\sigma}$ and also showing the result from the electronic localization function indicating higher π - than σ -aromaticity in Al_4^{2-} ,^{25b} but in contrast with the fact that the ring current in Al_4^{2-} has a negligible contribution from the two π -electron

system.^{16,23} For symmetry reasons, the MCI_{π} values of D_{4h} Al_4^{2-} and Ge_4^{2+} clusters with two π -electrons are exactly the same, 0.187 e. Total MCI and absolute NICS values are somewhat larger for Ge_4^{2+} , but this is, in part, the result of shorter Ge–Ge bond lengths. For comparison purposes, let us add here that the MCI and NICS(0) values for $D_{4h} C_4H_4^{2+}$,

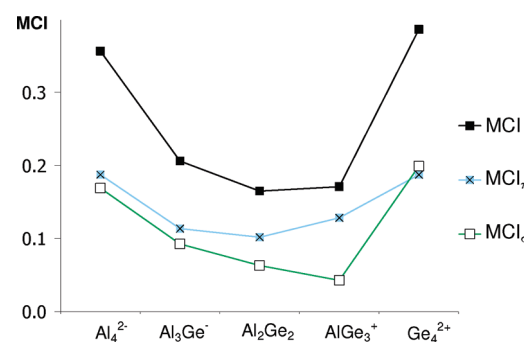


Figure 1. Variation of MCI, MCI_{π} , and MCI_{σ} (in electrons) along the series Al_4^{2-} , Al_3Ge^- , Al_2Ge_2 , $AlGe_3^+$, and Ge_4^{2+} .

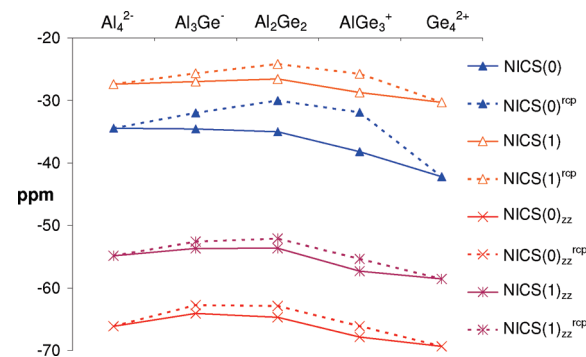


Figure 2. Comparison between NICS (ppm) indices calculated at the ring center and at the RCP (dotted line) along the series Al_4^{2-} , Al_3Ge^- , Al_2Ge_2 , $AlGe_3^+$, and Ge_4^{2+} .

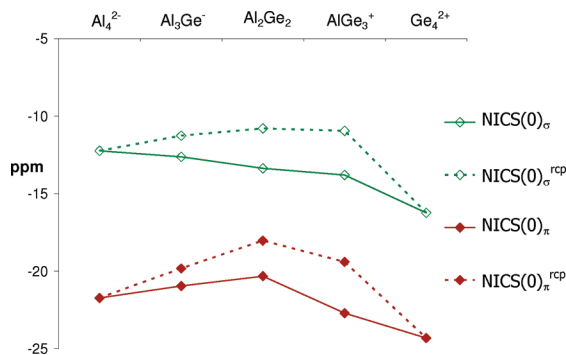


Figure 3. Comparison between dissected NICS (ppm) indices calculated at the ring center and at the RCP (dotted line) along the series Al_4^{2-} , Al_3Ge^- , Al_2Ge_2 , AlGe_3^+ , and Ge_4^{2+} .

the organic molecule being most comparable to Al_4^{2-} or Ge_4^{2+} , are 0.185 e and -15.62 ppm, respectively.

Figures 1 and 2 depict the trends observed along the series Al_4^{2-} to Ge_4^{2+} for the MCI and NICS indices, respectively. Interestingly, both total MCI and MCI_π curves have a clear concave U shape providing the expected order of aromaticity, i.e., $\text{Al}_4^{2-} > \text{Al}_3\text{Ge}^- \geq \text{Al}_2\text{Ge}_2 \leq \text{Al}\text{Ge}_3^+ < \text{Ge}_4^{2+}$. As to the NICS values, NICS(0) fails showing a steady increase of aromaticity along the Al_4^{2-} to Ge_4^{2+} series. Remarkably, NICS(0)^{rcp} yields the anticipated order of aromaticity,

indicating that the point selected to compute the NICS value in inorganic clusters may have a relevant influence in the aromaticity trends obtained. The distance between the geometrical ring center and the RCP is 0.19, 0.28, and 0.39 Å in Al_3Ge^- , Al_2Ge_2 , and AlGe_3^+ , respectively, showing significant differences of -2.58 , -4.99 , and -6.28 ppm between the NICS(0) and NICS(0)^{rcp}. Clearly, the RCP yields better results than the geometrical center of the ring for NICS(0). Minor changes in the out-of-plane component of the NICS(0) and NICS(0)_{zz}, computed in the ring center or in the RCP, were found. In both cases, NICS(0)_{zz} and NICS(0)_{zz}^{rcp}, the shape of the curve is close to the expected one with the only exception of the aromaticity of Al_3Ge^- , that is found to be slightly lower than that of Al_2Ge_2 . Moreover, NICS(1), NICS(1)^{rcp}, NICS(1)_{zz}, and NICS(1)_{zz}^{rcp} curves show the expected U behavior. These results oppose to previous claims asserting that NICS(0) is better suited than NICS(1) for the evaluation of aromaticity in all-metal clusters.^{5f}

Finally, dissected NICS calculations have been performed in order to study the trends of π - and σ -aromaticity (see Figures 3 and 4). Interestingly, NICS(0)_π and NICS(0)_σ calculated at the ring center show opposite trends. The first reproduces the predicted concave shape, while the latter exhibits a smooth increase of aromaticity from Al_4^{2-} to

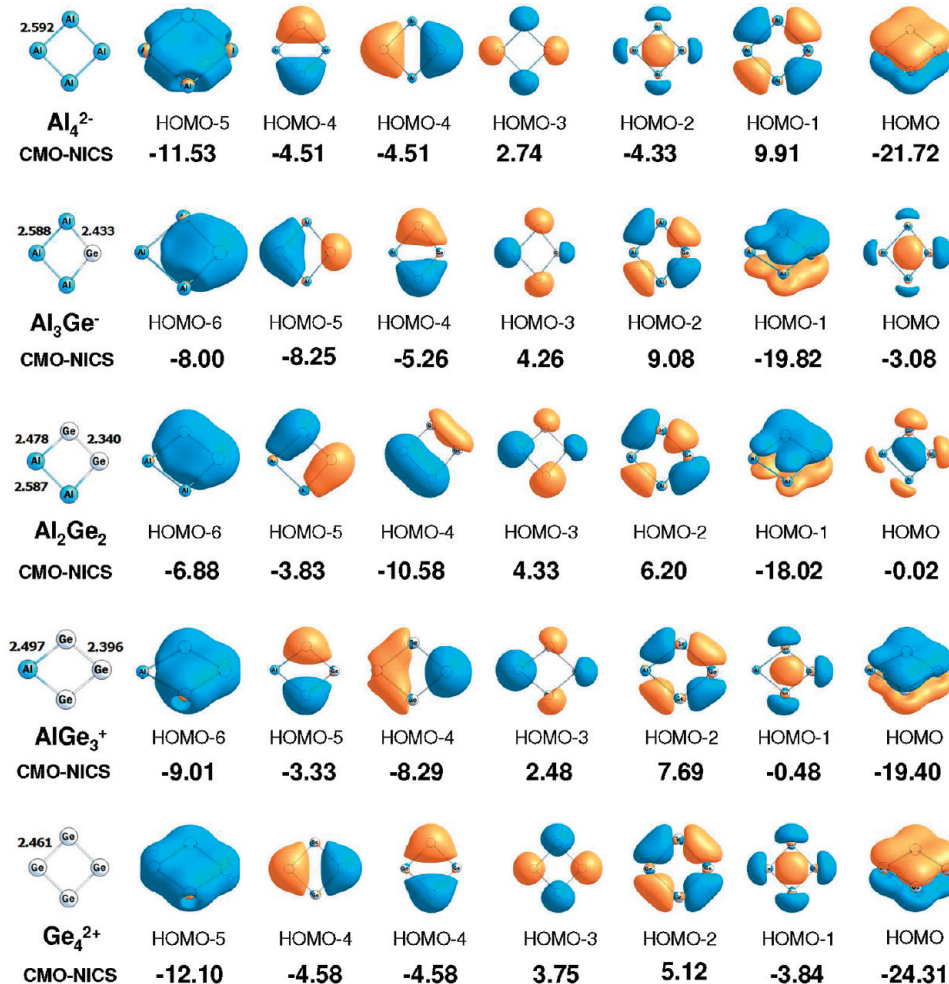


Figure 4. Canonical molecular orbital contribution to NICS(0)^{rcp} (ppm) for the series Al_4^{2-} , Al_3Ge^- , Al_2Ge_2 , AlGe_3^+ , and Ge_4^{2+} .

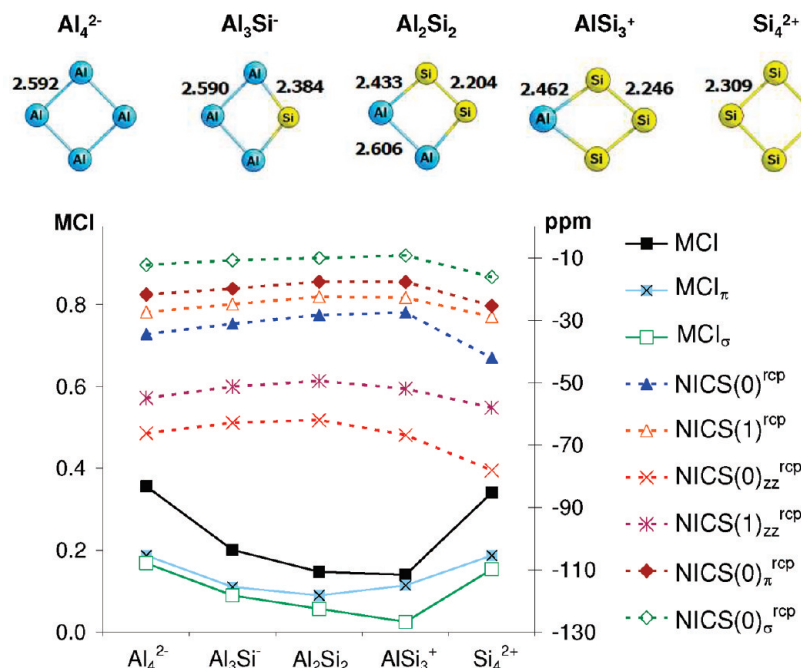


Figure 5. Variation of MCI, MCI_{π} , and MCI_{σ} (in electrons) and NICS (ppm) indices calculated at the RCP (dotted line) along the series Al_4^{2-} , Al_3Si^- , Al_2Si_2 , AlSi_3^+ , and Si_4^{2+} .

Ge_4^{2+} . This last behavior has been previously observed for NICS(0). Therefore, in this series, the σ contribution is responsible for the NICS(0) failing. On the other hand, as previously seen, NICS(0σ)^{rcp} provides the expected order, indicating that NICS(0σ) is more sensitive than NICS(0π) at the point where the NICS is computed. Figures 2 and 3 show the differences between the NICS measured at the ring center and at the RCP. In all cases, the latter reproduces properly the expected U shape. Consequently, here after, only the NICS indices calculated at the RCP will be taken into account. Moreover, in the next series, only the figures with selected MCI and NICS curves will be presented (see Supporting Information for tables with the complete set of results). Figure 4 depicts the valence orbitals with its individual contribution to NICS. Interestingly, the radial σ -orbital (HOMO-2 in Al_4^{2-}) reproduces the predicted concave shape, as does the total NICS(σ)^{rcp}, while the tangential σ -orbital (HOMO-1 in Al_4^{2-}) presents a different behavior. In the rest of this work, the individual contributions will only be used to explain the cases where NICS(σ) or NICS(π) fail.

Next, the remaining series where X and Y belong to different groups of the Periodic Table are briefly analyzed. The molecular structure, the MCI and NICS curves obtained for the 4-MR valence isoelectronic series $[\text{Al}_n\text{Si}_{4-n}]^{2-n}$ ($n = 0-4$) are depicted in Figure 5. Whereas MCI indicates somewhat larger aromaticity for Al_4^{2-} , all NICS indices give Si_4^{2+} as the most aromatic cluster. The trend obtained when going from Al_4^{2-} to Si_4^{2+} for all the studied indicators of total ($\sigma + \pi$) aromaticity is the same and corresponds to the expected one, except for NICS(0σ)^{rcp} and MCI that yield AlSi_3^+ slightly less aromatic than Al_2Si_2 . When the $\sigma-\pi$ separation is applied to the MCI and NICS(0σ)^{rcp} indices, it is found that MCI_{π} and NICS(0π)^{rcp} show the expected U shape, while MCI_{σ} and NICS(0σ)^{rcp} constantly decrease when going from Al_4^{2-} to AlSi_3^+ . Then the σ -aromaticity abruptly

increases from AlSi_3^+ to the full symmetric Si_4^{2+} . As it will be seen in the next series, MCI_{σ} and the absolute value of NICS(0σ)^{rcp} tend to decrease when group 13 atoms (Al, Ga) are substituted by group 14 atoms (Si, Ge), except when the D_{4h} structure is reached. In contrast to the previous series, the contribution of the radial σ -orbital to NICS increases when going from X_2Y_2 to XY_3^+ (see Figure 6). This fact leads to a slightly lower σ aromaticity in XY_3^+ than X_2Y_2 . However, this effect is, in most cases, canceled out by the π contribution when total MCI and NICS indices are analyzed, and consequently, the expected concave shape is observed.

After that we consider the two valence isoelectronic series $[\text{X}_n\text{Y}_{4-n}]^{2-n}$ (X = Ga and Y = Si and Ge; $n = 0-4$). Figures 7 and 8 depict the most relevant MCI and NICS curves obtained. Interestingly, almost all indices coincide in giving a similar aromaticity to Ga_4^{2-} and Ge_4^{2+} clusters, while MCI differs from NICS in giving somewhat larger aromaticity to Ga_4^{2-} than to Si_4^{2+} . In addition, all indices provide the expected U shape, except NICS(0σ)^{rcp}, NICS(0π)^{rcp}, and MCI_{σ} for the series $[\text{Ga}_n\text{Si}_{4-n}]^{2-n}$ ($n = 0-4$) that, as before, yield GaSi_3^+ , slightly less aromatic than Ga_2Si_2 . In the case of MCI, the decrease of σ -aromaticity in GaSi_3^+ is counteracted by MCI_{π} . In general, small differences between X_2Y_2 and XY_3^+ species are observed. For such cases, one cannot rule out the possibility that a change of method or basis set may lead to a different order of aromaticity.

Figure 9 collects the molecular structure, the MCI and the NICS values obtained for the valence isoelectronic series $[\text{Al}_n\text{Ga}_{4-n}]^{2-}$ ($n = 0-4$). In comparison with the previous series, changes in bond distances and angles are now smaller due to successive substitution of Al by Ga. The B3LYP/6-311+G(d) Ga–Ga bond distance of 2.568 Å found is not far from the 2.618 Å obtained at the CCSD(T)/6-311+G(d) level of theory^{26b} and from the 2.47 Å found in an organometallic compound synthesized by

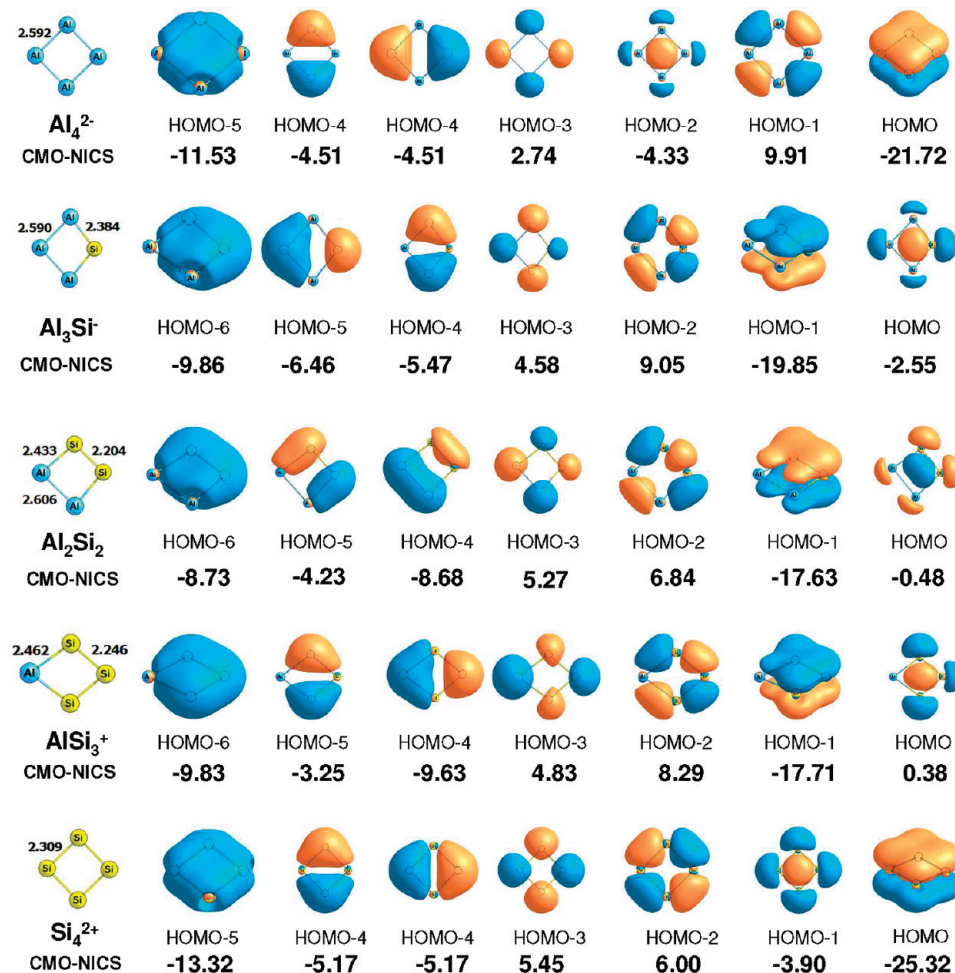


Figure 6. Canonical molecular orbital contribution to NICS(0)^{rcp} (ppm) for the series Al_4^{2-} , Al_3Si^- , Al_2Si_2 , AlSi_3^+ , and Si_4^{2+} .

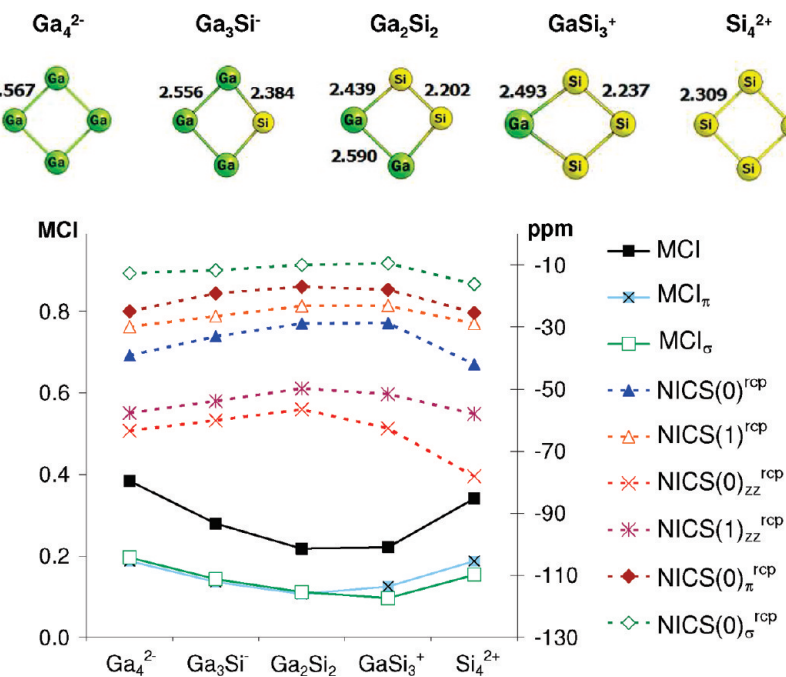


Figure 7. Variation of MCI, MCI_π , and MCI_σ (in electrons) and NICS (ppm) indices calculated at the RCP (dotted line) along the series Ga_4^{2-} , Ga_3Si^- , Ga_2Si_2 , GaSi_3^+ , and Ga_4^{2+} .

Twamley and Power^{26a} that contains the Ga_4^{2-} unit coordinated to two K^+ and bound diagonally to two phenyl carbons. Likewise, changes in aromaticity along the Al_4^{2-}

to Ga_4^{2-} series according to MCI and NICS results are relatively small. This is not unexpected taking into account that Ga and Al belong to group 13 and that the differences

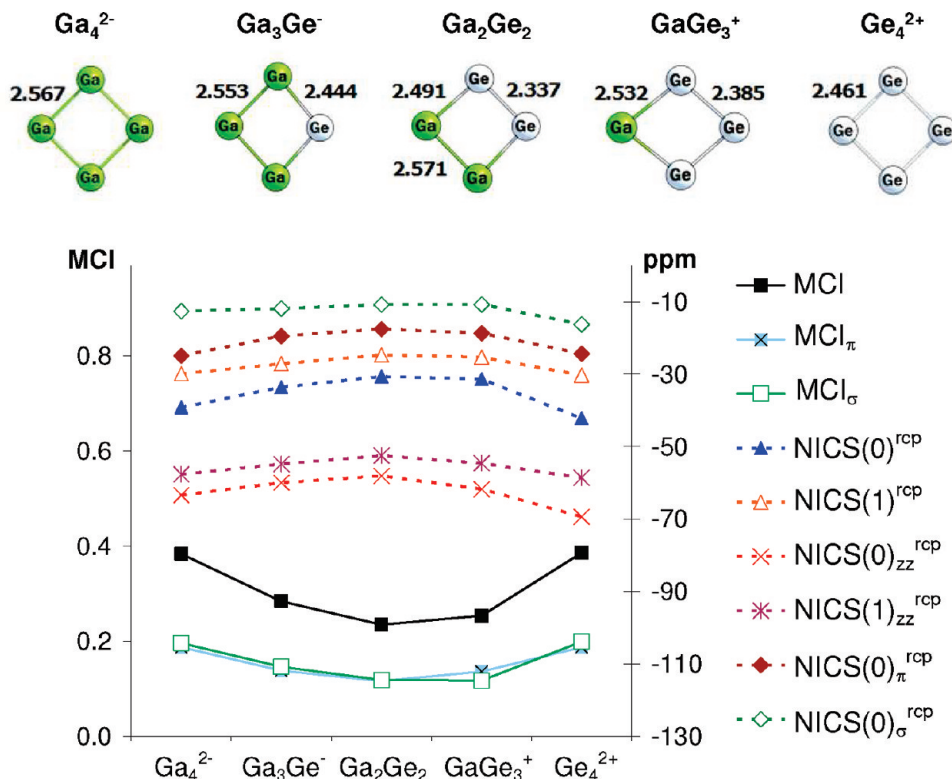


Figure 8. Variation of MCI, MCI_π , and MCI_σ (in electrons), and NICS (ppm) indices calculated at the RCP (dotted line) along the series Ga_4^{2-} , Ga_3Ge^- , Ga_2Ge_2 , GaGe_3^+ , and Ge_4^{2+} .

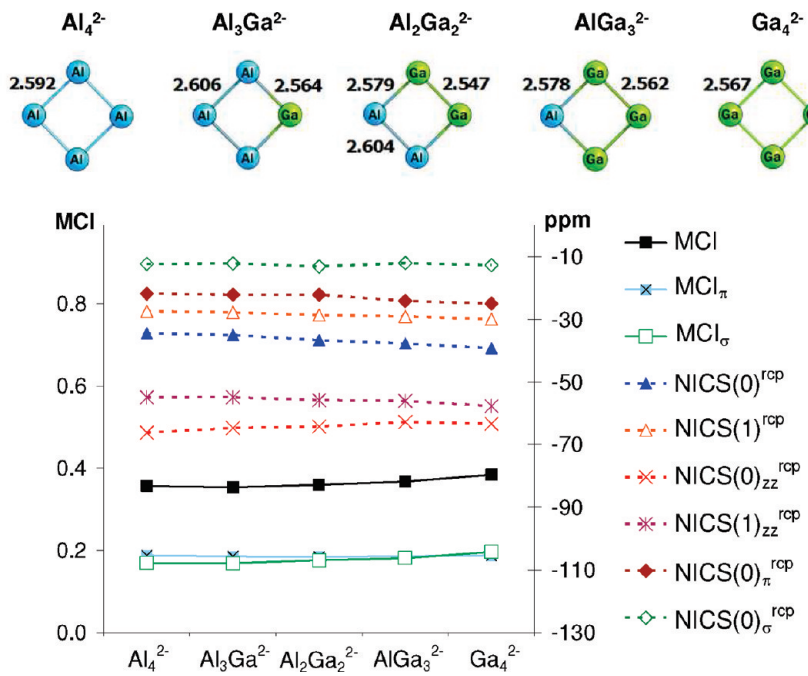


Figure 9. Variation of MCI, MCI_π , and MCI_σ (in electrons) and NICS (ppm) indices calculated at the RCP (dotted line) along the series Al_4^{2-} , $\text{Al}_3\text{Ga}^{2-}$, $\text{Al}_2\text{Ga}_2^{2-}$, $\text{Al}\text{Ga}_3^{2-}$, and Ga_4^{2-} .

of electronegativity between them are lower than those between Al and Ge or Si. MCI yields Al_4^{2-} slightly less aromatic than Ga_4^{2-} in disagreement with a crude evaluation of the resonance energy of Na_2Al_4 and Na_2Ga_4 by Boldyrev and Kuznetsov.¹⁰ These authors reported that the resonance energy of Na_2Al_4 compound is higher than that of the Na_2Ga_4 cluster by about 10 kcal·mol⁻¹. Correspondingly, NICS results predict higher aromaticity

for Ga_4^{2-} , except in the case of $\text{NICS}(0)_{zz}^{\text{rCP}}$. The trends of $\text{NICS}(0)^{\text{rCP}}$, $\text{NICS}(1)^{\text{rCP}}$, $\text{NICS}(1)_{zz}^{\text{rCP}}$, and $\text{NICS}(0)_\pi^{\text{rCP}}$ in Figure 9 show a steady increase of aromaticity from Al_4^{2-} to Ga_4^{2-} . MCI_π curve has a clear U shape, although it is less pronounced than in the previous series, providing the expected order of aromaticity, i.e., $\text{Al}_4^{2-} \geq \text{Al}_3\text{Ga}^{2-} \sim \text{Al}_2\text{Ga}_2^{2-} \sim \text{Al}\text{Ga}_3^{2-} \leq \text{Ga}_4^{2-}$. Finally, MCI and $\text{NICS}(0)_{zz}^{\text{rCP}}$ yield the correct trend except for $\text{Al}_2\text{Ga}_2^{2-}$

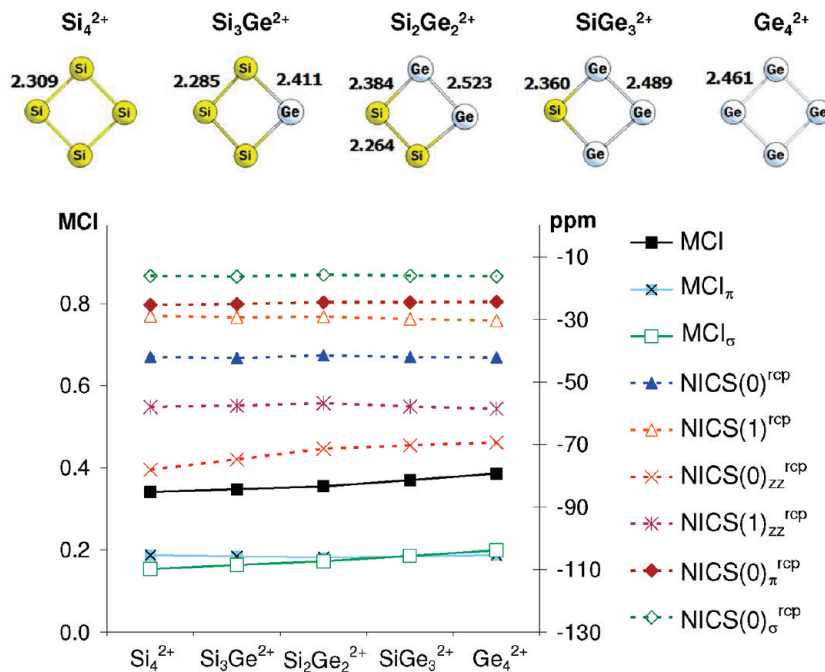


Figure 10. Variation of MCI, MCI_{π} , and MCI_{σ} (in electrons) and NICS (ppm) indices calculated at the RCP (dotted line) along the series Si_4^{2+} , $\text{Si}_3\text{Ge}^{2+}$, $\text{Si}_2\text{Ge}_2^{2+}$, $\text{Si}\text{Ge}_3^{2+}$, and Ge_4^{2+} .

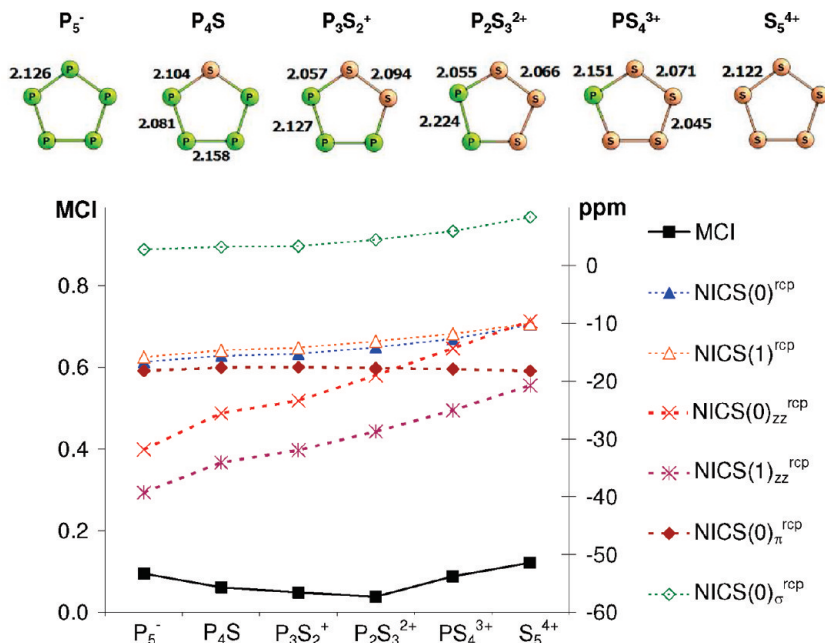


Figure 11. Variation of MCI, MCI_{π} , and MCI_{σ} (in electrons) and NICS (ppm) indices calculated at the RCP (dotted line) along the series P_5^- , P_4S , P_3S_2^+ , $\text{P}_2\text{S}_3^{2+}$, PS_4^{3+} , and S_5^{4+} .

that is found to be slightly more aromatic than $\text{Al}_3\text{Ga}^{2-}$ (MCI) or AlGa_3^{2-} (NICS(0_{zz})^{rcp}).

For the valence isoelectronic series $[\text{Si}_n\text{Ge}_{4-n}]^{2+}$ ($n = 0-4$), we have a similar situation as in the series Al_4^{2-} to Ga_4^{2-} . Thus, changes in bond distances and angles are small by successive substitution of Si by Ge atoms (see Figure 10). Likewise, changes in aromaticity along the Si_4^{2+} to Ge_4^{2+} series according to MCI and NICS results are generally minor. This is attributed again to the fact that Si and Ge belong to the same group 14 and that the electronegativities of Si and Ge are almost the same. All methods predict a slightly higher aromaticity for Ge_4^{2+}

as compared to Si_4^{2+} , except in the case of NICS(0_{zz})^{rcp} and NICS(0_{π})^{rcp}. As to the trends shown in Figure 10, only for MCI_{π} and NICS(1_{zz})^{rcp}, the curves have a clear concave shape providing the expected order of aromaticity, i.e., $\text{Si}_4^{2+} \geq \text{Si}_3\text{Ge}^{2+} \sim \text{Si}_2\text{Ge}_2^{2+} \sim \text{Si}\text{Ge}_3^{2+} \leq \text{Ge}_4^{2+}$. MCI indicates a steady increase of aromaticity along the Si_4^{2+} to Ge_4^{2+} series, while NICS(0_{zz})^{rcp} gives exactly the opposite trend. Finally, NICS(0)^{rcp}, NICS(1)^{rcp}, and NICS(0_{σ})^{rcp} show a tendency to increase from Si_4^{2+} to Ge_4^{2+} but present some oscillatory behavior. Results show that it is more difficult to observe a clear trend of aromaticity in the series with elements that belong to the

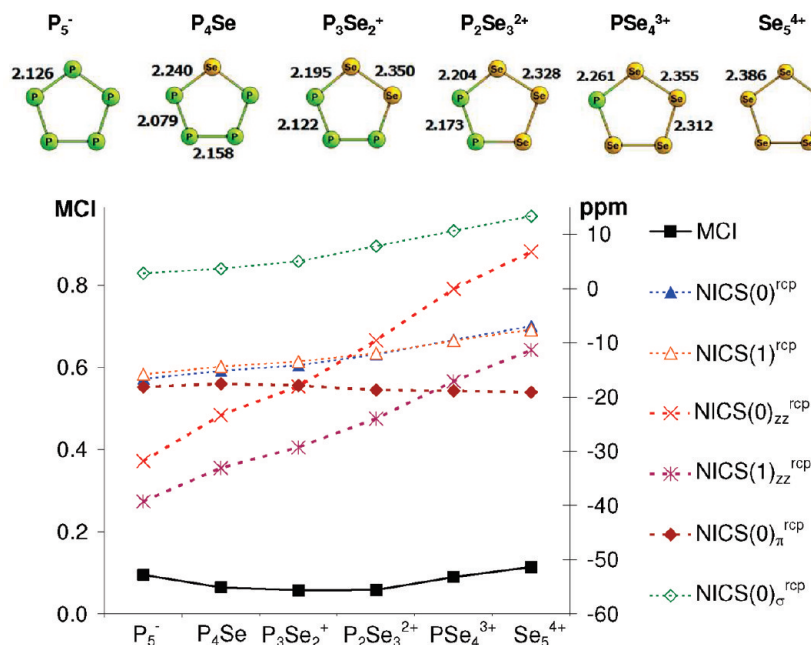


Figure 12. Variation of MCI, MCI_{π} , and MCI_{σ} (in electrons) and NICS (ppm) indices calculated at the RCP (dotted line) along the series P_5^- , P_4Se , $P_3Se_2^+$, $P_2Se_3^{2+}$, PSe_4^{3+} , and Se_5^{4+} .

Table 2. Summary of the Results Obtained at the B3LYP/6-311+G(d) Level for the Six Series Studied with Seven Descriptors of Aromaticity Analyzed

series	MCI	MCI_{π}	$NICS(0)^{rcp}$	$NICS(1)^{rcp}$	$NICS(0)_{zz}^{rcp}$	$NICS(1)_{zz}^{rcp}$	$NICS(0)_{\pi}^{rcp}$
Al/Ge	yes	yes	yes	yes	unclear ^a	yes	yes
Al/Si	unclear ^a	yes	unclear ^a	yes	yes	yes	yes
Ga/Si	yes	yes	unclear ^a	unclear ^a	yes	yes	yes
Ga/Ge	yes	yes	yes	yes	yes	yes	yes
P/S	yes	yes	no	no	no	no	yes
P/Se	yes	yes	no	no	no	no	unclear ^a

^a Fails only in ordering one molecule (see text).

same group of the Periodic Table. In these series, aromaticity remains basically unchanged by successive substitution. Due to the lack of a well-defined trend, these last two series should not be used as possible tests to evaluate the performance of aromaticity indices in all-metal clusters. Still, results indicate presumably, that the MCI_{π} index performs better than the rest for these two series.

Finally, we discuss the $[X_n Y_{5-n}]^{4-n}$ ($X = P$ and $Y = S$ and Se ; $n = 0-5$) series of 5-MR clusters. Figures 11 and 12 list the molecular structure, MCI, and NICS curves for these valence isoelectronic clusters. Since the D_{5h} rings of P_5^- , S_5^{4+} , and Se_5^{4+} have six π -electrons, it is not possible to derive the MCI_{π} value using simple algebra without computation. Among these series, P_5^- is the only inorganic cluster that has been studied previously with quantum mechanical methods.^{5e,30} These works show that D_{5h} P_5^- possess six π -electrons in three π molecular orbitals, resulting in π -aromaticity according to the $4n + 2$ Hückel's rule. In line with this view, the MCI and MCI_{π} values of P_5^- differ by only 0.001 e, indicating that the contribution of the σ -electrons to the total MCI value is irrelevant. The same is true for all the members of these two series. MCI values yield more aromatic S_5^{4+} and Se_5^{4+} clusters than P_5^- , while all NICS indices predict the opposite behavior. From the trends depicted in Figures 11 and 12, it is found that both

MCI and MCI_{π} curves present the expected \cup shape (MCI_{π} is not represented in Figures 11 and 12 because it coincides almost exactly with MCI). However, all NICS values yield a continuous reduction of aromaticity along the series P_5^- to S_5^{4+} and to Se_5^{4+} . Remarkably, $NICS(0)_{\pi}^{rcp}$ differs from the rest of NICS indices, showing the same behavior of MCI and MCI_{π} . $NICS(0)_{\pi}^{rcp}$ values yield more aromatic S_5^{4+} and Se_5^{4+} clusters than P_5^- and provide a clear \cup shape, with the only exception of P_4Se being a little less aromatic than $P_3Se_2^+$. On the other hand, σ -orbitals are responsible for the reduction of aromaticity that is shown by the rest of NICS indices along the series. For comparison purposes, the MCI and $NICS(0)$ values for D_{5h} $C_5H_5^-$, the most similar organic molecule to P_5^- , are 0.0704 e and -15.63 ppm, respectively.

4. Concluding Remarks

The summary of the results obtained for six of the series analyzed can be found in Table 2. In this table, we write “yes” when a certain index follows the expected trend in aromaticity for a given series, “no” otherwise, and “unclear” when the failure of the index is minor (for instance, the index fails short only for the ordering of one species in a given series). The series analyzed constitute a new test to evaluate the performance of descriptors of aromaticity in the exciting field of all-metal clusters.

Results in Table 2 indicate that the multicenter indices perform generally better than NICS, especially the MCI_{π} . Our results reinforce the superior behavior of $NICS(0)_{\pi}^{rcp}$ as compared to $NICS(0)^{rcp}$, $NICS(1)^{rcp}$ and their corresponding out-of-plane components. Indeed, $NICS(0)_{\pi}^{rcp}$ gives the correct trends for all studied species, except for the relative aromaticity of P_4Se in comparison with $P_3Se_2^+$, and for the valence isoelectronic series $[Al_nGa_{4-n}]^{2-}$ and $[Si_nGe_{4-n}]^{2+}$ ($n = 0-4$). These two latter series, for which only the MCI_{π} index yields the correct trend, have not been included in Table 2 because aromaticity results show that there is not a well-defined trend along these series. The fact that $NICS(0)_{\sigma}^{rcp}$ performs better than $NICS(0)^{rcp}$, $NICS(1)^{rcp}$, or their corresponding out-of-plane components for the $[X_nY_{4-n}]^{q\pm}$ ($X, Y = Al, Ga, Si, and Ge; n = 0-4$) clusters is somewhat disturbing given the fact that these molecules display both σ - and π -aromaticity. The reason must be found in the $NICS(0)_{\sigma}^{rcp}$ component that fails to account for the expected order of aromaticity. Remarkably, NICS values in inorganic aromatic clusters strongly depend on the point where they are calculated. Thus, while $NICS(0)^{rcp}$ provides the expected trend, $NICS(0)$ fails predicting a steady increase when going from Al_4^{2-} to Ge_4^{2+} .

NICS and MCI are indices of aromaticity that do not require reference values and, consequently, they are likely the most useful indicators of aromaticity for all-metal and semimetal clusters. The present study indicates that if one wants to order a series of inorganic compounds according to their aromaticity, it is recommendable to use multicenter electronic indices or $NICS(0)_{\pi}^{rcp}$ values. However, for this purpose neither NICS(0) nor NICS(1) are reliable. On the other hand, if one only wants to discuss whether a given cluster is aromatic or not, then both MCI and NICS, and particularly NICS-scan, do a good job to classify all-metal and semimetal clusters into aromatic, nonaromatic, and antiaromatic.²¹

Finally, the performance of NICS and MCI has been validated for the light atoms of Periodic Table, but still remain to be assessed for more complicated transition metals having δ - or ϕ -electron delocalization. More research is underway in our laboratory concerning this particular issue.

Acknowledgment. Financial help has been furnished by the Spanish MICINN project no. CTQ2008-03077/BQU and by the Catalan DIUE through project no. 2009SGR637. M.S. is indebted to the Catalan DIUE for financial support through the ICREA Academia Prize 2010. F.F. and J.P. thank the MICINN for the doctoral fellowship no. AP2005-2997 and the Ramón y Cajal contract, respectively. E.M. acknowledges financial support from the Lundbeck Foundation Center and from Marie Curie IntraEuropean Fellowship, Seventh Framework Programme (FP7/2007–2013), under grant agreement no. PIEF-GA-2008-221734. We thank the Centre de Supercomputació de Catalunya (CESCA) for partial funding of computer time.

Supporting Information Available: B3LYP/6-311+G(d) optimized Cartesian coordinates, the complete set of tables and dissected NICS for all the inorganic systems

discussed in this work are available. This material is available free of charge via the Internet at <http://pubs.acs.org>.

References

- (1) Li, X.; Kuznetsov, A. E.; Zhang, H.-F.; Boldyrev, A.; Wang, L.-S. *Science* **2001**, *291*, 859–861.
- (2) (a) Boldyrev, A. I.; Wang, L.-S. *Chem. Rev.* **2005**, *105*, 3716–3757. (b) Tsipis, C. A. *Coord. Chem. Rev.* **2005**, *249*, 2740–2762. (c) Zubarev, D. Y.; Averkiev, B. B.; Zhai, H.-J.; Wang, L.-S.; Boldyrev, A. I. *Phys. Chem. Chem. Phys.* **2008**, *10*, 257–267.
- (3) (a) Zhai, H. J.; Averkiev, B. B.; Zubarev, D. Y.; Wang, L.-S.; Boldyrev, A. I. *Angew. Chem., Int. Ed.* **2007**, *46*, 4277. (b) Averkiev, B. B.; Boldyrev, A. I. *J. Phys. Chem. A* **2007**, *111*, 12864–12866.
- (4) Tsipis, A. C.; Kefalidis, C. E.; Tsipis, C. A. *J. Am. Chem. Soc.* **2008**, *130*, 9144–9155.
- (5) (a) Kuznetsov, A. E.; Boldyrev, A. I.; Li, X.; Wang, L.-S. *J. Am. Chem. Soc.* **2001**, *123*, 8825–8831. (b) Kuznetsov, A. E.; Corbett, J. D.; Wang, L.-S.; Boldyrev, A. I. *Angew. Chem., Int. Ed. Engl.* **2001**, *40*, 3369–3372. (c) Zhan, C.-G.; Zheng, F.; Dixon, D. A. *J. Am. Chem. Soc.* **2002**, *124*, 14795–14803. (d) Zhai, H.-J.; Kuznetsov, A. E.; Boldyrev, A.; Wang, L.-S. *ChemPhysChem* **2004**, *5*, 1885–1891. (e) Liu, Z.-Z.; Tian, W.-Q.; Feng, J.-K.; Zhang, G.; Li, W.-Q. *J. Phys. Chem. A* **2005**, *109*, 5645–5655. (f) Chi, X. X.; Chen, X. J.; Yuan, Z. S. *J. Mol. Struct. (Theochem)* **2005**, *732*, 149–153.
- (6) (a) Lin, Y. C.; Jusélius, J.; Sundholm, D.; Gauss, J. *J. Chem. Phys.* **2005**, *122*, 214308. (b) Islas, R.; Heine, T.; Merino, G. *J. Chem. Theory Comput.* **2007**, *3*, 775–781. (c) Kuznetsov, A. E.; Birch, K. A.; Boldyrev, A. I.; Zhai, H.-J.; Wang, L.-S. *Science* **2003**, *300*, 622–625. (d) Ugrinov, A.; Sen, A.; Reber, A. C.; Qian, M.; Khanna, S. N. *J. Am. Chem. Soc.* **2008**, *130*, 782–783.
- (7) (a) Kruszewski, J.; Krygowski, T. M. *Tetrahedron Lett.* **1972**, *13*, 3839–3842. (b) Krygowski, T. M. *J. Chem. Inf. Comp. Sci.* **1993**, *33*, 70–78.
- (8) Matito, E.; Duran, M.; Solà M. *J. Chem. Phys.* **2005**, *122*, 014109. Erratum: *J. Chem. Phys.* **2006**, *125*, 059901.
- (9) Cyrański, M. K. *Chem. Rev.* **2005**, *105*, 3773–3811.
- (10) Boldyrev, A. I.; Kuznetsov, A. E. *Inorg. Chem.* **2002**, *41*, 532–537.
- (11) (a) Hückel, E. *Z. Physik* **1931**, *70*, 204–286. (b) Hückel, E. *Z. Physik* **1931**, *72*, 310–337. (c) Hückel, E. *Z. Physik* **1932**, *76*, 628–648. (d) Hückel, E. *Z. Elektrochem.* **1937**, *43*, 752–788, and 827–849.
- (12) Schleyer, P. v. R.; Maerker, C.; Dransfeld, A.; Jiao, H.; van Eikema Hommes, N. J. R. *J. Am. Chem. Soc.* **1996**, *118*, 6317–6318.
- (13) (a) Giambiagi, M.; de Giambiagi, M. S.; dos Santos, C. D.; de Figueiredo, A. P. *Phys. Chem. Chem. Phys.* **2000**, *2*, 3381–3392. (b) Bultinck, P.; Ponec, R.; Van Damme, S. *J. Phys. Org. Chem.* **2005**, *18*, 706–718. (c) Bultinck, P.; Rafat, M.; Ponec, R.; van Gheluwe, B.; Carbó-Dorca, R.; Popelier, P. *J. Phys. Chem. A* **2006**, *110*, 7642–7648.
- (14) (a) Mandado, M.; Krishtal, A.; Van Alsenoy, C.; Bultinck, P.; Hermida-Ramón, J. M. *J. Phys. Chem. A* **2007**, *111*, 11885–11893. (b) Roy, D. R.; Bultinck, P.; Subramanian, V.; Chattaraj, P. K. *J. Mol. Struct. (Theochem)* **2008**, *854*, 35–39. (c) Jiménez-Halla, J. O. C.; Matito, E.; Blancafort, L.; Robles, J.; Solà, M. *J. Comput. Chem.* **2009**, *30*, 2764–2776.

- (15) (a) Havenith, R. W. A.; Fowler, P. W.; Steiner, E.; Shetty, S.; Kanhere, D.; Pal, S. *Phys. Chem. Chem. Phys.* **2004**, *6*, 285–288. (b) Jung, Y.; Heine, T.; Schleyer, P. v. R.; Head-Gordon, M. *J. Am. Chem. Soc.* **2004**, *126*, 3132–3138.
- (16) Fowler, P. W.; Havenith, R. W. A.; Steiner, E. *Chem. Phys. Lett.* **2001**, *342*, 85–90.
- (17) Havenith, R. W. A.; van Lenthe, J. H. *Chem. Phys. Lett.* **2004**, *385*, 198–201.
- (18) Aihara, J.; Kanno, H.; Ishida, T. *J. Am. Chem. Soc.* **2005**, *127*, 13324–13330.
- (19) Corminboeuf, C.; Heine, T.; Weber, J. *Phys. Chem. Chem. Phys.* **2003**, *5*, 246–251.
- (20) (a) Chen, Z.; Corminboeuf, C.; Heine, T.; Bohmann, J.; Schleyer, P. v. R. *J. Am. Chem. Soc.* **2003**, *125*, 13930–13931. (b) Wannere, C. S.; Corminboeuf, C.; Wang, Z.-X.; Wodrich, M. D.; King, R. B.; Schleyer, P. v. R. *J. Am. Chem. Soc.* **2005**, *127*, 5701–5705.
- (21) Jiménez-Halla, J. O. C.; Matito, E.; Robles, J.; Solà, M. J. *Organomet. Chem.* **2006**, *691*, 4359–4366.
- (22) Tsipis, A. C. *Phys. Chem. Chem. Phys.* **2009**, *11*, 8244–8261.
- (23) Fowler, P. W.; Havenith, R. W. A.; Steiner, E. *Chem. Phys. Lett.* **2002**, *359*, 530–536.
- (24) Feixas, F.; Matito, E.; Poater, J.; Solà, M. J. *Comput. Chem.* **2008**, *29*, 1543–1554.
- (25) (a) Jusélius, J.; Straka, M.; Sundholm, D. *J. Phys. Chem. A* **2001**, *105*, 9939–9944. (b) Santos, J. C.; Tiznado, W.; Contreras, R.; Fuentealba, P. *J. Chem. Phys.* **2004**, *120*, 1670–1673. (c) Chatarraj, P. K.; Roy, D. R.; Elango, M.; Subramanian, V. *J. Phys. Chem. A* **2005**, *109*, 9590–9597.
- (26) (a) Twamley, B.; Power, P. P. *Angew. Chem., Int. Ed. Engl.* **2000**, *39*, 3500–3503. (b) Kuznetsov, A. E.; Boldyrev, A. I.; Li, X.; Wang, L.-S. *J. Am. Chem. Soc.* **2001**, *123*, 8825–8831.
- (27) (a) Li, X.; Zhang, H.-F.; Wang, L.-S.; Kuznetsov, A. E.; Cannon, N. A.; Boldyrev, A. I. *Angew. Chem., Int. Ed. Engl.* **2001**, *40*, 1867–1870. (b) Yang, L.-M.; Wang, J.; Ding, Y.-H.; Sun, C.-C. *Organometallics* **2007**, *26*, 4449–4455.
- (28) (a) Seal, P. *J. Mol. Struct. (Theochem)* **2009**, *893*, 31–36. (b) Nigam, S.; Majumder, C.; Kulshreshtha, S. K. *J. Mol. Struct. (Theochem)* **2005**, *755*, 187–194.
- (29) Chi, X. X.; Li, X. H.; Chen, X. J.; Yuang, Z. S. *J. Mol. Struct. (Theochem)* **2004**, *677*, 21–27.
- (30) (a) Jin, Q.; Jin, B.; Xu, W. G.; Zhu, W. *J. Mol. Struct. (Theochem)* **2005**, *713*, 113–117. (b) Kraus, F.; Korber, N. *Chem.—Eur. J.* **2005**, *11*, 5945–5959. (c) De Proft, F.; Fowler, P. W.; Havenith, R. W. A.; Schleyer, P. v. R.; Van Lier, G.; Geerlings, P. *Chem.—Eur. J.* **2004**, *10*, 940–950.
- (31) Frisch, M. J.; Trucks, G. W.; Schlegel, H. B.; Scuseria, G. E.; Robb, M. A.; Cheeseman, J. R.; Montgomery Jr., J. A.; Vreven, T.; Kudin, K. N.; Burant, J. C.; Millam, J. M.; Iyengar, S. S.; Tomasi, J.; Barone, V.; Mennucci, B.; Cossi, M.; Scalmani, G.; Rega, N.; Petersson, G. A.; Nakatsuji, H.; Hada, M.; Ehara, M.; Toyota, K.; Fukuda, R.; Hasegawa, J.; Ishida, M.; Nakajima, T.; Honda, Y.; Kitao, O.; Nakai, H.; Klene, M.; Li, X.; Knox, J. E.; Hratchian, H. P.; Cross, J. B.; Bakken, V.; Adamo, C.; Jaramillo, J.; Gomperts, R.; Stratmann, R. E.; Yazyev, O.; Austin, A. J.; Cammi, R.; Pomelli, C.; Ochterski, J. W.; Ayala, P. Y.; Morokuma, K.; Voth, G. A.; Salvador, P.; Dannenberg, J. J.; Zakrzewski, G.; Dapprich, S.; Daniels, A. D.; Strain, M. C.; Farkas, O.; Malick, D. K.; Rabuck, A. D.; Raghavachari, K.; Foresman, J. B.; Ortiz, J. V.; Cui, Q.; Baboul, A. G.; Clifford, S.; Cioslowski, J.; Stefanov, B. B.; Liu, G.; Liashenko, A.; Piskorz, P.; Komaromi, I.; Martin, R. L.; Fox, D. J.; Keith, T.; Al-Laham, M. A.; Peng, C. Y.; Nanayakkara, A.; Challacombe, M.; Gill, P. M. W.; Johnson, B.; Chen, W.; Wong, M. W.; Gonzalez, C.; Pople, J. A. *Gaussian 03*, revision C.01; Gaussian, Inc.: Pittsburgh, PA, 2003.
- (32) Stephens, P. J.; Devlin, F. J.; Chabalowski, C. F.; Frisch, M. J. *J. Phys. Chem.* **1994**, *98*, 11623–11627.
- (33) Becke, A. D. *J. Chem. Phys.* **1993**, *98*, 5648–5652.
- (34) Lee, C.; Yang, W.; Parr, R. G. *Phys. Rev. B: Condens. Matter Mater. Phys.* **1988**, *37*, 785–789.
- (35) (a) Krishnan, R.; Binkley, J. S.; Seeger, R.; Pople, J. A. *J. Chem. Phys.* **1980**, *72*, 650–654. (b) Frisch, M. J.; Pople, J. A.; Binkley, J. S. *J. Chem. Phys.* **1984**, *80*, 3265–3269.
- (36) Lambrecht, D. S.; Fleig, T.; Sommerfeld, T. *J. Phys. Chem. A* **2008**, *112*, 2855–2862.
- (37) Zubarev, D. Y.; Boldyrev, A. I. *J. Phys. Chem. A* **2008**, *112*, 7984–7985.
- (38) Lambrecht, D. S.; Fleig, T.; Sommerfeld, T. *J. Phys. Chem. A* **2008**, *112*, 7986–7986.
- (39) (a) Wolinski, K.; Hilton, J. F.; Pulay, P. *J. Am. Chem. Soc.* **1990**, *112*, 8251–8260. (b) Cheeseman, J. R.; Trucks, G. W.; Keith, T. A.; Frisch, M. J. *J. Chem. Phys.* **1996**, *104*, 5497–5509.
- (40) Bader, R. F. W. *Atoms in Molecules: A Quantum Theory*; Oxford University Press; Oxford, U.K., 1990.
- (41) (a) Cossio, F. P.; Morao, I.; Jiao, H. J.; Schleyer, P. v. R. *J. Am. Chem. Soc.* **1999**, *121*, 6737–6746. (b) Morao, I.; Lecea, B.; Cossio, F. P. *J. Org. Chem.* **1997**, *62*, 7033–7036.
- (42) Schleyer, P. v. R.; Manoharan, M.; Wang, Z. X.; Kiran, B.; Jiao, H. J.; Puchta, R.; van Eikema Hommes, N. J. R. *Org. Lett.* **2001**, *3*, 2465–2468.
- (43) Corminboeuf, C.; Heine, T.; Seifert, G.; Schleyer, P. v. R.; Weber, J. *Phys. Chem. Chem. Phys.* **2004**, *6*, 273–276.
- (44) (a) Glendening, E. D.; Badenhoop, J. K.; Reed, A. E.; Carpenter, J. E.; Bohmann, J. A.; Morales, C. M.; Weinhold, F. *NBO 5.0 Program*; Theoretical Chemistry Institute, University of Wisconsin, Madison, WI, 2001; (b) Reed, A. E.; Curtiss, L. A.; Weinhold, F. *Chem. Rev.* **1988**, *88*, 899–926.
- (45) Cioslowski, J.; Matito, E.; Solà, M. *J. Phys. Chem. A* **2007**, *111*, 6521–6525.
- (46) (a) Mandado, M.; González-Moa, M. J.; Mosquera, R. A. *J. Comput. Chem.* **2007**, *28*, 127–136. (b) Mandado, M.; González-Moa, M. J.; Mosquera, R. A. *ChemPhysChem* **2007**, *8*, 696–702.
- (47) (a) Matito, E.; Solà, M.; Salvador, P.; Duran, M. *Faraday Discuss.* **2007**, *135*, 325–345. (b) Matito, E.; Poater, J.; Solà, M.; Duran, M.; Salvador, P. *J. Phys. Chem. A* **2005**, *109*, 9904–9910. (c) Ponec, R.; Cooper, D. *J. Mol. Struct. (Theochem)* **2005**, *727*, 133–138.
- (48) (a) Bader, R. F. W. *Acc. Chem. Res.* **1985**, *18*, 9–15. (b) Bader, R. F. W. *Chem. Rev.* **1991**, *91*, 893–928.
- (49) Biegler-König, F. W.; Bader, R. F. W.; Tang, T.-H. *J. Comput. Chem.* **1982**, *3*, 317–328. (<http://www.chemistry.mcmaster.ca/aimpac/>).
- (50) Matito, E. *ESI-3D: Electron Sharing Indexes Program for 3D Molecular Space Partitioning*; Institute of Computational

- Chemistry, University of Girona: Catalonia, Spain, 2006;
<http://iqc.udg.es/~eduard/ESI>.
- (51) The numerical accuracy of the QTAIM calculations has been assessed using two criteria: (i) The integration of the Laplacian of the electron density ($\nabla^2\rho(\mathbf{r})$) within an atomic basin must be close to zero; and (ii) The number of electrons in a molecule must be equal to the sum of all the electron populations of the molecule. For all atomic calculations, integrated absolute values of $\nabla^2\rho(\mathbf{r})$ were always less than 0.001 au. For all molecules, errors in the calculated number of electrons were always below 0.01 au. It is important to mention that the default maximum distance from the nucleus used to integrate the atomic region has to be increased when diffuse functions are employed in the presence of metal atoms. In the AIMPAC program, the default integration maximum distance is 9.0 au. However, we have found that this distance should be increased to 12.0 au for the proper integration of Al and Ge atoms, and to 17.0 au for Ga. If this value is not increased, the sum of all electron populations will not be equal to the number of electrons in a molecule. Consequently, these integration distances have to be changed in the input file.
- (52) The reason for the differences found is not totally clear to us, although it may be the result of using the default maximum distance (9 au) for the integration of the atomic regions in the AIMPAC program instead of our recommended value of 12 au for Al.
- (53) Feixas, F.; Matito, E.; Solà, M.; Poater, J. *J. Phys. Chem. A* **2008**, *112*, 13231–13238.

CT100034P